

# Melt Damage to Gas Nozzle Tip in Close-Coupled Gas Atomization

N. Kato<sup>1</sup>, T. Ohmura<sup>1</sup>, T. Maruyama<sup>1</sup>, Y. Hamada<sup>1</sup> and T. Shakouchi<sup>2\*</sup>

1: Fukuda Metal Foil & Powder Co., Ltd., Japan

2: Mie University, Japan

\* Correspondent author: shako@mach.mie-u.ac.jp

## Abstract

One of the methods for producing metal fine powder is gas atomization. When a supersonic under-expanded gas jet from an annular nozzle is ejected near the molten metal from a concentric circular nozzle placed in the direction of gravity, the molten metal splits into droplets which is broken up just after the nozzle exit and is further miniaturized in the jet shear layer. It is then cooled to produce fine metal powder of several microns to several tens of microns. The gas jet flows from an annular nozzle while enclosing a negative pressure recirculating vortex region, and a high temperature molten metal flows into this region. In a close-coupled gas atomizer, the gas nozzle tip may be damaged by molten metal if the protrusion length of the molten metal delivery nozzle is short. In this study, the mechanism of melt damage of gas nozzle tip in close-coupled gas atomizer and preventive measures are examined by numerical and experimental analyses.

**Keyword:** Gas atomization, Supersonic under-expanded jet, Reattached jet, Melt damage, Flow control

## 1. Introduction

In a gas atomization method for producing fine metal powder, a supersonic under-expanded gas jet issued from an annular nozzle is generally used. Here, molten metal from the melt delivery nozzle at the centre is introduced into the recirculating vortex region with a large negative pressure and into the shear layer with a large velocity gradient of supersonic under-expanded jet issued from an annular nozzle. Consequently, the molten metal splits into droplets, which is broken up just after the nozzle exit, further miniaturized by a large shear force in the shear layer, and turns into small droplets, micro particles, and fine powder. The flow is extremely complex and unstable because the supersonic annular jet flows under a free boundary including the vortex region and there are a hot molten metal in the flow field and divisions and phase change from the liquid metal to fine solid particles.

Many studies on gas atomization have been conducted. Lubanska [1] demonstrated the atomization characteristics of some liquid metals that were gas-atomized using spray rings as well as the approximate correlation between the particle median diameter and mass ratio of the metal to gas flow. Ünal [2] studied the production of aluminium alloy powder by gas atomization using a close-coupled gas atomizer and estimated the flow pattern using gas atomization of water. Fukuda [3] studied experimentally the velocity distribution of a confined-type gas atomization nozzle. Figliora and Anderson [4] investigated numerically how melt tube geometry influences the gas flow field of a high pressure gas atomizer. Anderson and Tepstra [5] studied the effect of operating gas pressure for various nozzles on the gas mass flow rate and size distribution of 316L stainless steel atomized. Ting et al. [6] investigated the jet pulsation of an atomizer by analysing high speed images and showed that the atomizer plume oscillated with two dominant frequencies of 10 and 1200 Hz. A 304L stainless steel alloy was atomized at the supply pressure of  $P_0 = 6.5$  MPa using argon gas. Motaman et al. [7] studied an optimum arrangement by changing the injection angle of a gas nozzle at  $P_0 = 1.0$  MPa relative to the melt delivery nozzle of a close-coupled gas atomizer to avoid melt damage of the gas nozzle. The gas nozzle consisted of an 18 hole discrete gas jet die configuration. Two-dimensional numerical analysis and flow visualization were carried out, and they showed the mechanism of the melt damage of the gas nozzle tip. Zhao et al. [8] demonstrated the primary atomization process by a close-coupled gas atomizer

using numerical analysis. However, they did not consider the breakup of the molten metal. The effects of operational parameters on the particle size distribution were also investigated by many researchers [9].

In the present study, the flow characteristics of a supersonic under-expanded air jet from an annular nozzle are examined using a numerical analysis, and the characteristics are compared with the visualized flow pattern of gas atomization of water using a two-dimensional experimental test model. In gas atomization, generally, the maximum supply pressure of gas is as large as  $P_0 = 0.5$  MPa, however, here it is mainly kept at relatively low pressure of  $P_0 = 0.4$  MPa. Operating the atomizer at low pressure is also important from the view point of energy and resource savings. The behaviour of the molten metal flow is simulated using atomized water flow [2]. In addition, gas atomization of molten copper at  $1400^\circ\text{C}$  and  $P_0 = 0.4$  MPa is also carried out, and the effects of the geometry of the flow passage on the melting damage of the air nozzle tip is examined precisely relative to the flow characteristics using numerical and experimental analyses.

## 2. Numerical Analysis

The flow field in gas atomization is very complex because it is three dimensional, compressible, unsteady, and is a three-phase flow, including the phase change from liquid metal to fine solid particles. Therefore, exactly analysing the flow field is extremely difficult. In this study, to understand the flow field of gas atomization numerical analysis of a compressible high speed gas jet flow is conducted using the computational fluid dynamics (CFD) program FlowSimulation. In the CFD program, the governing equations are obtained using the  $k-\epsilon$  turbulence model. The governing equation is a conservation law for mass, angular momentum, and energy. For the coordinate system, the Cartesian coordinates that rotate at angular velocity with respect to the axis passes through the origin of the coordinate system are used. The Favre-averaged Navier-Stokes equation is analysed based on the finite sedimentation and participation method. The three-dimensional calculation was carried out, and after the effects of the number of cells on the flow have been investigated,  $4.15 \times 10^6$  cells are used.

## 3. Experimental Apparatus and Procedure

### 3.1 Two-dimensional axisymmetric model and gas atomization of water

Figure 1 shows the two-dimensional axisymmetric experimental model and apparatus for the gas atomization of water. The model was designed to simulate the gas atomization of copper, as will be explained later. It had a simple geometry, and the air nozzle axis was parallel to the axis of the melt delivery nozzle. It consisted of two nozzle walls and upper and lower end plates. A water nozzle was installed at the centre. The arrangement of the nozzles was axisymmetric. The nozzle wall and endplate were made of brass

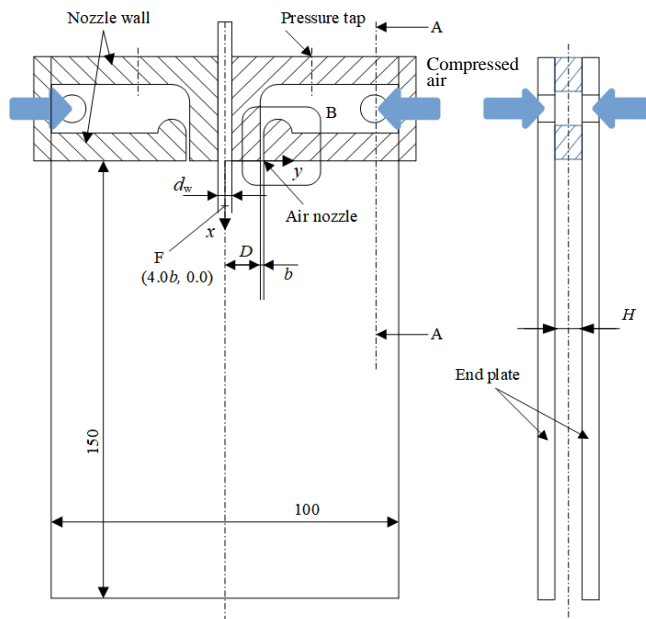


Fig. 1. Experimental apparatus of gas atomization [position of pressure sensor, F: (4.0b, 0.0)]

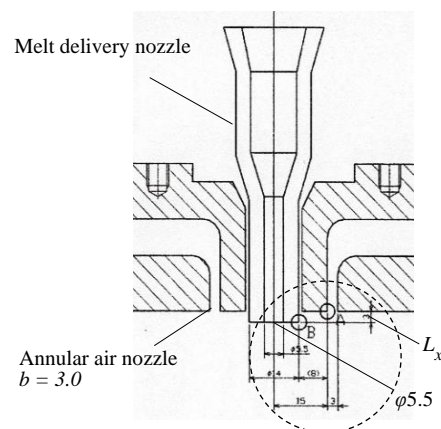


Fig. 2. Gas atomization nozzle for copper ( $b = 3.0$  mm,  $D/b = 5.0$ ,  $d_m = 5.5$  mm.  $L_x/b$ : changed from 0 to 10)

## Melt Damage to Gas Nozzle Tip in Close-coupled Gas Atomization

and transparent acrylic resin, respectively. The air from the compressor flowed through the reservoir, regulator, dryer, and flow meter (AZBIL, Air flow monitor, Japan, GMG500) and into the apparatus. An equal amount of compressed air was introduced through four 8.5 mm diameter inflow holes located at the upper and lower end plates. Water was supplied from the centre nozzle after the flow rate has been measured. The volumetric flow rate of water was the same as that of the gas atomization of copper. The widths of the air and water nozzles were  $b = 2.5$  and  $d_w = 4.58$  mm, respectively, and the height of the nozzles was  $H = 5.0$  mm. The offset distance is  $D/b = 5.0$ . Two 0.8 mm diameter static holes were installed at the centre height of the nozzle wall before the air nozzle, which were used to measure supply pressure  $P_0$ . The supply pressure varied up to a maximum value of  $P_0 = 0.5$  MPa, and flow visualization, velocity measurement, and pressure measurement were carried out. The behaviour of the water flow was recorded using a video camera (Sony, Japan, FDR-AX45). Pitot tubes with 1.0 mm diameter, which measured the total and static pressures, were used to measure the velocity at the centre plane of the apparatus. The velocity distribution was obtained using the total and static pressure measurements by considering the compressibility of air. A three-dimensional traverse device was used to move the Pitot tube. The pressure was measured using a Bourdon tube and mercury column manometers, and the fluctuating pressure at position F ( $4.0b, 0.0$ ) (shown in Fig. 1) was measured using a pressure transducer (JTEKT, Japan, PD104K-100K).

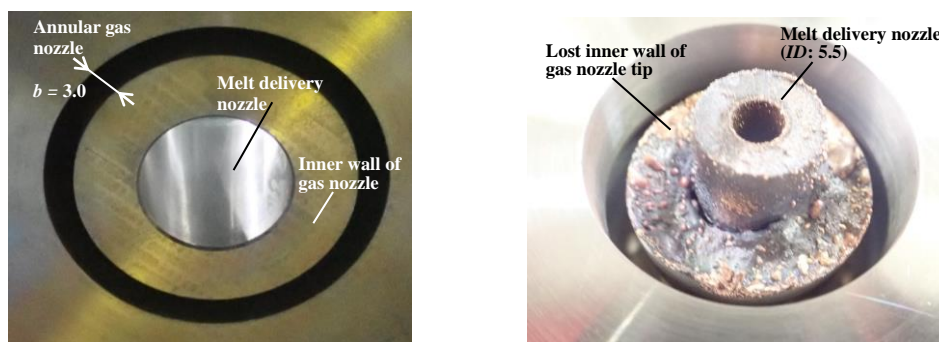
### 3.2 Gas atomization of copper

Gas atomization of copper was carried out. The nozzles used are shown in Figure 2. The exit diameter of the melt delivery nozzle and width of the annular air nozzle were  $d_m = 5.5$  and  $b = 3.0$  mm, respectively. The offset distance is  $D/b = 5.0$ . The protrusion length could be varied from  $L_x/b = 0$  to 10. Molten copper at 1400 °C was supplied at a rate of 50 kg/180 s, and the supply pressure of air was varied from  $P_0 = 0.4$  to 0.5 MPa. The air and melt delivery nozzles were made of SUS-630 stainless steel, fine ceramics. The size distribution of the product was analysed using the laser diffraction and scattering method (Malvern Panalytical division of Spectris Co., Ltd. Mastersizer 3000).

## 4. Results and Discussions

### 4.1 Gas atomization of copper and melting damage of air nozzle tip

We conduct the gas atomization experiment using the close-coupled gas atomizer at  $L_x/b = 1.0$ , as shown in Fig.2. The air supply pressure is  $P_0 = 0.4$  MPa, and copper at 1400 °C is supplied at 50 kg/180 s from the melt delivery nozzle with diameter  $d_m = 5.5$  mm. Figure 3 shows the melt delivery nozzle made of fine ceramics and the air nozzle made of stainless steel SUS-630 after the gas atomization of copper. The inner wall of the air nozzle is melted about 5 mm from the tip, which we considered to be due to the high temperature copper droplets that touch the tip of the air nozzle, as earlier mentioned.



(a) before the gas atomization experiment (b) after the gas atomization experiment

Fig. 3. Melt damage of gas nozzle tip ( $P_0 = 0.4$  MPa,  $L_x/b = 1.0$ )

### 4.2 Effect of protrusion length, $L_x$ , of melt delivery nozzle

We prevent the melting damage of the inner tip wall of the air nozzle by letting the molten metal nozzle protrude and changing the jet flow pattern from the air nozzle.

Figure 4(a) shows the three-dimensional numerical results of the velocity distribution in the  $x$ - $y$  plane around the annular nozzle exit (in Fig. 2, the area indicated by the dashed circle) and the flow pattern was axisymmetric.  $P_0 = 0.4$  MPa, and the protrusion length of the melt delivery nozzle is  $L_x/b = 3.0$ . This is the result for air flow. The red coloured region shows the expansion and high speed area. The jet from the

annular nozzle forms the first, second, and third shock cells. However, the jet does not adhere to the side wall, and a reverse flow occurs around the corner (C in the figure) of the melt delivery nozzle to the tip of the gas nozzle. The arrows show the approximate flow direction. The droplets of molten metal reach the tip of the gas nozzle following the reverse flow and flow fluctuation and subsequently melt the tip. As previously mentioned, the jet and atomized water flow with large fluctuation and high frequencies, which implies that the droplets in the atomized flow might have increased the chances of shifting into a reverse flow. Figure 4(b) shows the visualized flow pattern of the gas atomization of water. The white coloured area presents the atomized water flow. In this case, atomized water flow can be observed in the area between the jet and side wall of the melt delivery nozzle. The qualitative flow pattern is similar to that of air flow shown in Fig. 4(a). Figure 4(c) shows the pressure distribution. The dark-blue-coloured area shows the negative low pressure. The expansion area of the shock cell has the negative low pressure, and the compression area presents positive high pressure. The area between the jet and side wall of the melt delivery nozzle has relatively negative low pressure.

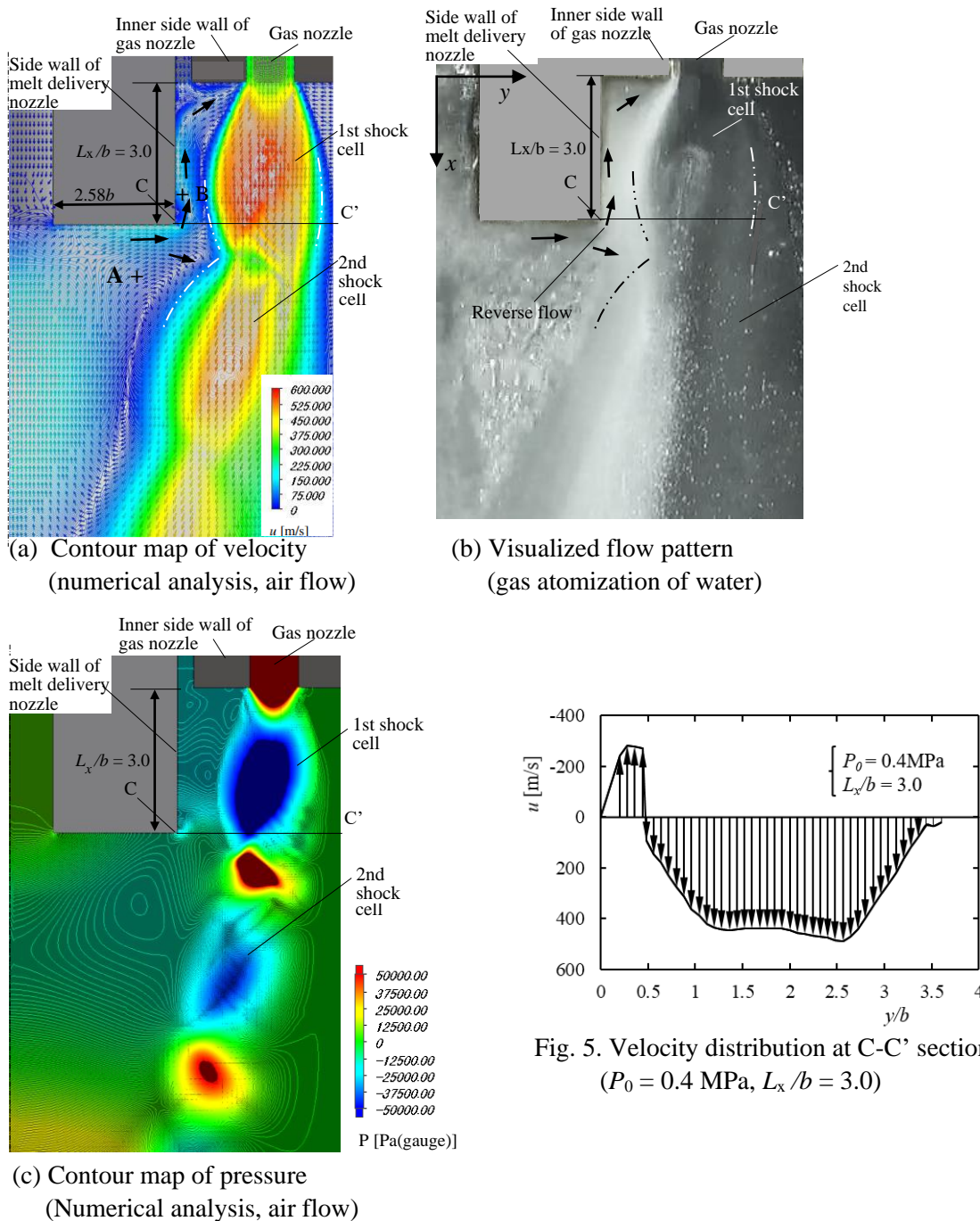


Fig. 4. Velocity and pressure distributions and flow visualization around nozzle exit ( $P_0 = 0.4 \text{ MPa}$ ,  $L_x/b = 3.0$ )

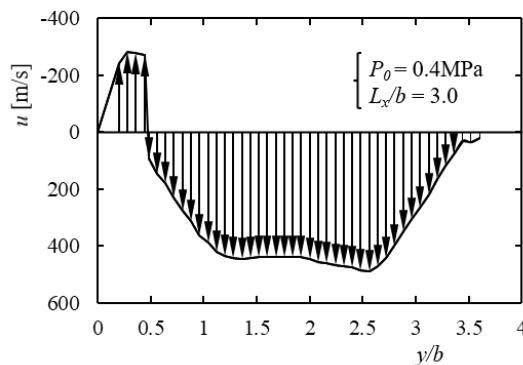


Fig. 5. Velocity distribution at C-C' section ( $P_0 = 0.4 \text{ MPa}$ ,  $L_x/b = 3.0$ )

## Melt Damage to Gas Nozzle Tip in Close-coupled Gas Atomization

Figure 5 shows the velocity distribution along the line C-C' around corner C shown in Fig. 4(a), which is measured using the total and static pressure Pitot tubes. The positive velocity indicates the flow toward main stream (x-direction), and the negative one in the area  $y/b < 0.5$  indicates a reverse flow. To prevent the reverse flow and melting damage of the air nozzle tip, we need to extend the protrusion length of the melt delivery nozzle.

Figure 6(a) shows the results at  $L_x/b = 5.67$ . In this case, the separating or reattaching stream line from the inner lip of the air nozzle reattaches at the side wall (R.P. in the figure) of the melt delivery nozzle that encloses the separating vortex region. This is the result for air flow. No flow occurs from the corner C to the vortex region, as shown in Fig. 4. This condition means that the melt droplets do not enter the region between the side wall of melt delivery nozzle and jet. Thus, the air nozzle tip does not melt. Figure 6(b) shows the visualized flow pattern of the gas atomization of water. The white coloured area presents the

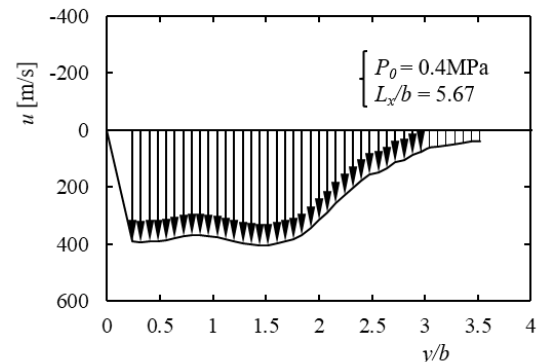
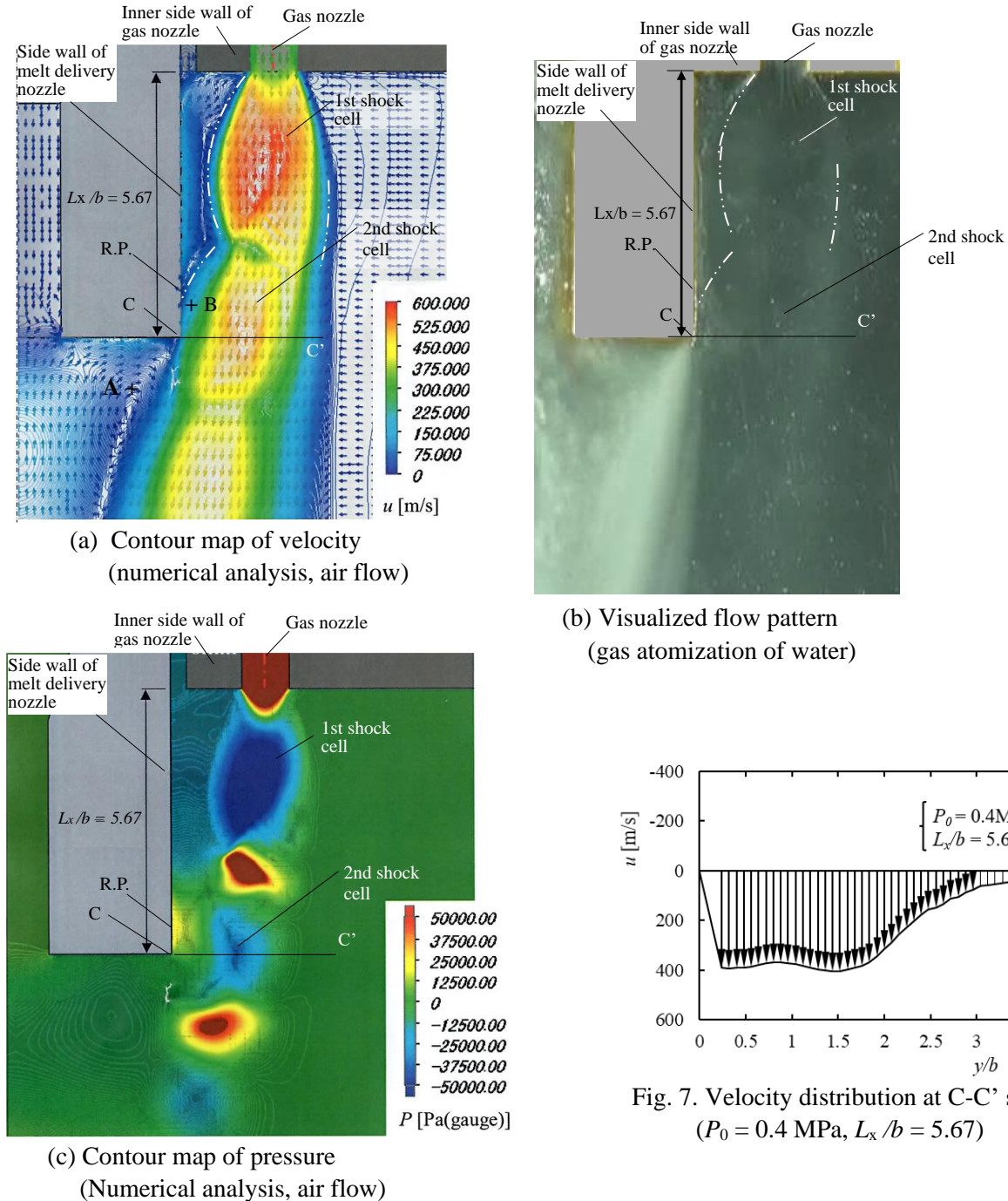


Fig. 7. Velocity distribution at C-C' section ( $P_0 = 0.4 \text{ MPa}$ ,  $L_x/b = 5.67$ )

Fig. 6. Velocity and pressure distributions and flow visualization around nozzle exit ( $P_0 = 0.4 \text{ MPa}$ ,  $L_x/b = 5.67$ )

atomized water flow. In this case, the jet reattaches to the side wall, and atomized water flow cannot be observed in the recirculating vortex region between the jet and side wall of the melt delivery nozzle. Figure 6(c) shows the pressure distribution. The increased pressure around corner C appears due to the jet reattachment.

Figure 7 shows the velocity distribution in line C-C' shown in Fig. 4(a). All values are positive, indicating that no reverse flow occurs. When  $L_x/b$  is larger than approximately 5.0, the nozzle tip is believed to do not melt.

Figure 8 shows the size distribution of the products of the gas atomization experiment of copper. The size distribution ranges from 4.0 to 700  $\mu\text{m}$ , and median diameter  $d_{50} = 86.0 \mu\text{m}$ . The sharpness is  $K = d_{75}/d_{50} = 4.0$ .

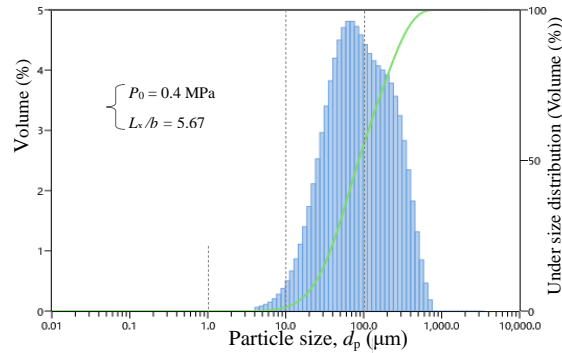


Fig. 8. Size distribution of products by gas atomization of copper ( $P_0 = 0.4 \text{ MPa}$ ,  $L_x/b = 5.67$ )

## 5. Conclusion

The melt damage of gas nozzle tip in close-coupled gas atomization was examined by experimental and numerical analyses.

The major results are as follows,

1. The mechanism of melting of gas nozzle tip was clarified through experimental and numerical analyses.
2. Melting of the gas nozzle tip can be prevented by setting the protrusion length of the molten metal nozzle,  $L_x$ , to  $L_x/b > 5.0$  when  $P_0 = 0.4$  to  $0.5 \text{ MPa}$ .
3. Control of particle size distribution of the product is a topic for future study.

## References

- [1] Lubanska H., "Correlation of spray ring data for gas atomization of liquid metals", *J. of Materials*, 22-2 (1970), pp. 45-49. <https://doi.org/10.1007/BF03355938>
- [2] Ünal A., "Production of rapidly solidified aluminium alloy powders by gas atomization and their applications", *Powder Metallurgy*, 33-1 (1990), pp. 53-64. <https://doi.org/10.1179/pom.1990.33.1.53>
- [3] Fukuda T., "Gas velocity distribution for a confined-type gas atomization nozzle (in Japanese)", *Tetsu-to-Hagane, J. of the Iron and Steel Institute of Japan*, 82-8 (1996), pp. 635-640. [https://doi.org/10.2355/tetsutohagane1955.82.8\\_635](https://doi.org/10.2355/tetsutohagane1955.82.8_635)
- [4] Mi J., Figliola R.S. and Anderson I.E., "A numerical investigation of gas flow effects on high pressure gas atomization to melt tip geometry variation", *Metallurgical and Materials Transactions B*, 28B (1997), pp. 935-941 <https://doi.org/10.1007/s11663-997-0021-7>.
- [5] Anderson I.E. and Tepstra R.I., "Progress toward gas atomization processing with increased uniformity and control", *Materials Science and Engineering A*, 326-1 (2002), pp. 101-109. [https://doi.org/10.1016/S0921-5093\(01\)01427-7](https://doi.org/10.1016/S0921-5093(01)01427-7)
- [6] Ting, J., Connor J. and Ridder S., "High speed cinematography of gas-metal atomizer", *Science and Engineering A*, 390 (2005) 452-460. <https://doi.org/10.1016/j.msea.2004.08.060>
- [7] Motaman S., Mullis A.M., Cochrane R.F., McCarthy I.N. and Borman D.J., "Numerical and experimental modelling of back stream flow during close-coupled gas atomization", *Computers & Fluids*, 88 (2013), pp. 1-10. <https://doi.org/10.1016/j.compfluid.2013.08.006>
- [8] Zhao W., Cao F., Ning Z., Li Z. and Sun J., "A computational fluid dynamics (CFD) investigation of the flow field and the primary atomization of the close coupled atomizer", *J. of Computers and Chemical Engineering*, 40 (2012), pp. 58-66. <https://doi.org/10.1016/j.compchemeng.2012.02.014>
- [9] Thompson J.S., Hasson O., Rolland S.A., Sienz J. and LSN Diffusion Ltd., "The identification of an accurate simulation approach to predict the effect of operational parameters on the particle size distribution (PSD) of powders produced by an industrial close-coupled gas atomiser", *Powder Technology*, 291 (2016), pp. 75-85. <https://doi.org/10.1016/j.powtec.2015.12.001>